Published in final edited form as:
Biomaterials. 2013 January ; 34(4): 912–921. doi:10.1016/j.biomaterials.2012.10.020.

Engineering Cell-Material Interfaces for Long-term Expansion of Human Pluripotent Stem Cells

Chien-Wen Chang[a,c,1], **Yongsung Hwang**[a,1], **Dave Brafman**[b,1], **Thomas Hagan**[a], **Catherine Phung**[b], and **Shyni Varghese**[a,*]

[a]Department of Bioengineering, University of California, San Diego, CA 92093, USA

[b]Department of Cellular and Molecular Medicine, University of California, San Diego, CA 92093, USA

Abstract

Cost-effective and scalable synthetic matrices that support long-term expansion of human pluripotent stem cells (hPSCs) have many applications, ranging from drug screening platforms to regenerative medicine. Here, we report the development of a hydrogel-based matrix containing synthetic heparin-mimicking moieties that supports the long-term expansion of hPSCs (≥20 passages) in a chemically defined medium. HPSCs expanded on this synthetic matrix maintained their characteristic morphology, colony forming ability, karyotypic stability, and differentiation potential. We also used the synthetic matrix as a platform to investigate the effects of various physicochemical properties of the extracellular environment on the adhesion, growth, and self-renewal of hPSCs. The observed cellular responses can be explained in terms of matrix interface-mediated binding of extracellular matrix proteins, growth factors, and other cell secreted factors, which create an instructive microenvironment to support self-renewal of hPSCs. These synthetic matrices, which comprise of “off-the-shelf” components and are easy to synthesize, provide an ideal tool to elucidate the molecular mechanisms that control stem cell fate.

*Corresponding author. Department of Bioengineering, University of California San, Diego, 9500 Gilman Drive, MC 0412, La Jolla, CA 92093, United States. Fax: +1 858 534 5722; svarghese@ucsd.edu (S. Varghese).
[c]Current address: Department of Biomedical Engineering and Environmental Sciences, National Tsing Hua University, Taiwan
[1]C.C, Y.H, and D.B contributed equally to this work

The authors declare no conflict of interest.

Author Contributions

C. W and S.V. conceptualized the study. C.W, Y.H, D.B., and S.V, designed the experiments, and analyzed the data. C.W., Y.H., D.B., T.H., and C.P performed the experiments. C.W., Y.H, D.B., and S.V contributed to the data interpretation, discussion, and writing the manuscript.

Supplementary Information

Supplementary Tables S1–S3
Supplementary Figures S1–S7

Keywords

human pluripotent stem cells; embryonic stem cells; self-renewal; hydrogels; synthetic matrices; physicochemical cues; synthetic heparin mimics

1. Introduction

Since the isolation of human embryonic stem cells (hESCs), there has been a tremendous interest in developing defined, scalable *in vitro* culture conditions that can support their growth. These efforts have led to the development of multiple defined growth media, but these still require either feeder layers such as mouse embryonic fibroblasts (MEFs) or biologically derived matrices such as Matrigel for maintenance of pluripotency and self-renewal of hPSCs(1–6). Development of chemically defined matrices is a challenging task because the myriad of physicochemical signals that MEFs and Matrigel provide. Within these limitations, recent advances in the field of biomaterials have led to identification of substrates—both naturally derived and synthetic—for the self-renewal of hPSCs(7–16). High-throughput screening technologies have contributed significantly towards the development of these chemically defined, synthetic materials(10, 17).

Accumulating evidence suggests that heparin molecules play a key role in maintaining self-renewal of hPSCs(4, 12, 18). Studies by Levenstein et al. showed the role of MEF-secreted heparan sulfate proteoglycans on self-renewal of hESCs(18). To harness the beneficial effects of heparin moieties on the self-renewal of hPSCs, Klim et al. have developed synthetic matrices that display heparin-binding peptides to support long-term self-renewal of hPSCs(12). The role of heparin moieties in self-renewal of hPSCs is not surprising given that heparin molecules can bind to soluble bFGF molecules and modulate their bioactivity(19–21); bFGF is a crucial biomolecule required for maintenance of self-renewal of hPSCs *in vitro*. Additionally, heparin molecules have been shown to protect bFGF from denaturation and proteolytic degradation, thereby increasing its longevity and function(21, 22).

Recently we have shown that synthetic heparin mimics such as poly(sodium-4-styrenesulfonate) (PSS) can bind to soluble bFGF and regulate FGF signaling akin to heparin molecules(19). Based on these findings along with the known role of bFGF molecules on *in vitro* self-renewal of hPSCs, we developed synthetic hydrogels containing PSS moieties to support long-term culture of hPSCs while maintaining their pluripotency. Employing hydrogel-based synthetic matrices, we further elucidated the role of physicochemical cues of the matrix on self-renewal of hPSCs. Such easy-to-synthesize and cost-effective synthetic matrices would not only accelerate the translational potential of hPSCs, but also provide a platform to decipher the interplay between various physicochemical cues on self-renewal of hPSCs. Additionally, these matrices would help to identify the myriad of molecular and signaling pathways that dictate stem cell fate and commitment.

2. Materials and Methods

2.1. Materials

N-acryloyl amino acid (AA) monomers, such as N-acryloyl 2-glycine (A2AGA), N-acryloyl 4-aminobutyric acid (A4ABA), N-acryloyl 6-aminocaproic acid (A6ACA), and N-acryloyl 8-aminocaprylic acid (A8ACA), were synthesized from glycine (Fisher Scientific, Inc.), 4-aminobutyric acid, 6-aminocaproic acid, and 8-aminocaprylic acid (Acros Organics Inc.), respectively, as described elsewhere(23). Sodium 4-vinylbenzenesulfonate (SS), 3-sulfopropyl acrylate potassium salt (SPA), and [2-(methacryloyloxy)ethyl]dimethyl-(3-sulfopropyl)ammonium hydroxide (MEDSAH) were purchased from Aldrich. Acrylamide (Am) was purchased from Invitrogen and N,N'-methylenebisacrylamide (BisAm), ammonium persulfate (APS) and N,N,N',N'-tetramethylethylenediamine (TEMED) were obtained from Sigma. The monomers used in this study are summarized in Supplementary Table S1.

2.2. Hydrogel synthesis

The hydrogels containing varying functional groups and hydrophilicity were synthesized through copolymerization of acrylamide with monomers containing either carboxylate or sulfonate groups. The PSS-based hydrogels (PAm_6-co-PSS_2, PAm_6-co-PSS_1, PAm_6-co-$PSS_{0.5}$,) were synthesized by copolymerizing acrylamide (Am, 7.5 mmol) with sodium 4-vinylbenzenesulfonate (SS, 2.5 mmol) at 6:2, 6:1, and 6:0.5 mole ratios. The monomers were dissolved in deionized (DI) water, and polymerized in BioRad 1 mm spacer glass plates at room temperature using 0.26, 0.19, and 0.10 mmol of BisAm as a crosslinker and 1.3% w/v of APS/TEMED (redox initiator/accelerator). Hydrogels containing SPA and MEDSAH moieties (PAm_6-co-$PSPA_2$, PAm_6-co-$PMEDSAH_2$) were synthesized by copolymerizing Am (7.5 mmol) with SPA (2.5 mmol) or MEDSAH (2.5 mmol) at a mole ratio of 6:2. The precursors were dissolved in DI water and polymerized using 0.26 mmol of BisAm and 1.3% w/v of APS/TEMED. Lastly, hydrogels with carboxyl groups were synthesized by copolymerizing Am (7.5 mmol) with AA monomers (2.5 mmol) at a mole ratio of 6:2 as described elsewhere (23). Briefly, the monomers were dissolved in 1 M NaOH and polymerized using 0.26 mmol of BisAm and 1.3% w/v of APS/TEMED. The compositions and nomenclature of the hydrogels are summarized in Supplementary Table S2. The hydrogels were sterilized with 70% ethanol and washed with fresh phosphate buffered saline (PBS) solution for 72 hrs. The rinsed hydrogels were incubated in culture media (high glucose DMEM with 2 mM L-glutamine and 50 units/ml penicillin/streptomycin) containing 10% fetal bovine serum (premium select) overnight before plating the cells.

2.3. Surface roughness

Surface roughness of hydrogels was evaluated using a Multimode AFM equipped with a Nanoscope IIIA controller from Veeco Instruments (Santa Barbara, CA) run by Nanoscope software v5.30 as previously reported (23). AFM images were acquired in contact mode at forces of ~4 nN with an "E" scanner (maximum scan area 12 × 12 mm^2) using Si3N4 cantilevers (Veeco) with 0.06 N/m nominal spring constants. Hydrogels were prepared as described above. Upon synthesis, hydrogels were washed in PBS for 36 hrs to leach out

unreacted reactants and to reach equilibrium swelling. For a given scan area, the reported roughness value is the average root mean square (RMS) roughness obtained from two different spots of triplicate samples. Using the nanoscope software data analysis was carried out where a flattening order 3 was applied to all images to correct for tilt and bow before roughness analysis.

2.4. Elastic modulus

Equilibrium swollen hydrogels in PBS were used for compression measurements (24). The measurements were performed using Bose ElectroForce 3200 Test Instrument (*Bose*, Minnesota, USA). Samples were compressed by two parallel plates at a maximum loading of 225 N with a crosshead speed of 0.1 mm/min. The elastic moduli were calculated from the linear region of the stress-strain curve (0–5% strain). All measurements were carried out as quadruplicates for each set of parameters.

2.5. Water contact angle

The water contact angle of the hydrogels was determined by a sessile drop method at room temperature using a contact angle meter (CAM100, KSV Instruments Ltd.) (23). A 5 μL droplet of water was placed on the surface of hydrogels. All samples were prepared as triplicates and results were shown as a mean value with standard deviation.

2.6. HUES9-Oct4-GFP

The lentiviral construct that was used to generate the Oct4-GFP reporter line was kindly provided by Dr. Alexey Terskikh. The reporter line was generated as described earlier (14). In short, the HUES9 cells were infected overnight with lenti Oct4-GFP and single clones were isolated and screened for stable GFP expression levels.

2.7. Culture of hPSCs

HUES9, HUES9-Oct4-GFP, HUES6, and hiPSC were expanded in defined medium (StemPro; DMEM/F-12 supplemented with StemPro supplement, 2% bovine serum albumin (BSA), 55 μM 2-mercaptoethanol, and 1% Gluta-MAX) or in MEF-conditioned medium. The MEF conditioned medium was collected after culturing MEF for 24 hrs using growth medium (Knockout DMEM supplemented with 10% Knockout Serum Replacement, 10% human plasmonate (Talecris Biotherapeutics), 1% non-essential amino acids, 1% penicillin/streptomycin, 1% Gluta-MAX, and 55 μM 2-mercaptoethanol) as described elsewhere(14). The hPSCs were cultured on mitotically inactivated MEF at an initial seeding density of 10^4 cells/cm^2 in MEF-conditioned medium prior to their culture on Matrigel or synthetic matrices. The hPSCs were manually passaged as small clumps of 30–40 μm size after 6 days of culture onto different matrices (Matrigel and synthetic matrices) by using a splitting ratio of 1:4. All the sequential passages were carried out similarly by passaging the cells manually. The hPSCs on PAm_6-co-PSS_2 hydrogels were passaged after 10–12 days depending upon the colony size and morphology. All cultures were supplemented with fresh medium containing 30 ng/ml of bFGF (Life Technologies) daily.

2.8. Population doubling time

Population doubling time (PDT) of HUES9 cells grown on Matrigel, MEF, and PAm_6-co-PSS_2 hydrogel was calculated using the equation below (15):

$$PDT(hr) = \frac{(T2 - T1)}{3.32 * (\log N2 - \log N1)}$$

where T1 and T2 represents days 3 and 5, respectively; N1 and N2 are the number of cells at T1 and T2, respectively. The number of cells at each time point was counted using TC10™ Automated Cell Counter.

For PDT measurements, HUES9 cells were cultured as single cells by enzymatically splitting the cells using Accutase. The cell count was carried out after 3 and 5 days of culture to calculate the population doubling time.

2.9. Immunocytochemistry

Immunofluorescent staining was performed using the following primary antibodies: OCT4 (1:200; Santa Cruz), NANOG (1:200; Santa Cruz), SOX17 (1:200; R & D systems), SMA (1:500; R & D systems), and NESTIN (1:50; BD Biosciences). The following secondary antibodies were used: goat anti-rabbit Alexa 647 (1:400; Life Technologies), donkey anti-mouse Alexa 546 (1:250; Life Technologies), and donkey anti-goat Alexa 546 (1:250; Life Technologies). For immunofluorescent staining, cells were fixed in 4% PFA for 5 min at 4°C, followed by 10 min at room temperature. Immediately before staining, the cells were permeabilized with 0.2% (v/v) Triton X-100 and blocked with 1% (w/v) BSA and 3% (w/v) nonfat dry milk for 30 min. Cells were stained with primary antibodies diluted in 1% BSA overnight at 4°C, washed 3 times with TBS, and incubated with secondary antibodies for 1 hr at 37°C. The nuclei were stained with Hoechst 33342 (2 μg/ml; Life Technologies) for 5 min at room temperature. Imaging was performed using an automated confocal microscope (Olympus Fluoview 1000 with motorized stage and incubation chamber).

2.10. RNA isolation and quantitative PCR

RNA isolation was carried out by using TRIzol (Invitrogen), and treated with DNase I (Invitrogen). Reverse transcription was performed by using qScript cDNA Supermix (Quanta Biosciences). Quantitative PCR was carried out by using TaqMan probes (Applied Biosystems) and TaqMan Fast Universal PCR Master Mix (Applied Biosystems) on a 7900HT Real Time PCR machine (Applied Biosystems). Taqman gene expression assay primers (Applied Biosystems) listed in Supplementary Table S3 were used. Gene expression was normalized to 18S rRNA levels. Delta Ct values were calculated as $\mathrm{C_t^{target}} - \mathrm{C_t^{18s}}$. All experiments were performed with three biological replicates.

2.11. FACS analysis

HPSCs were dissociated with Accutase. The cells were re-suspended in buffer (2% FBS/ 0.09% sodium azide/DPBS; BD Biosciences) and stained directly with Alexa-647 conjugated Tra-1-81 (Biolegend) or Alexa Fluor 647 mouse IgM,κ isotype control. Cells

were stained for 30 min on ice, washed, and re-suspended in buffer. Samples were analyzed by using BD Biosystems FACSCanto.

2.12. Embryoid body formation

The hPSCs cultured on PAm_6-co-PSS_2 were Accutased for 2–3 minutes and re-suspended in growth medium without the supplementation of bFGF, plated onto ultra low attachment plates, and cultured in 37°C/5% CO_2 incubator for 8 day to form embryoid body (EBD).

2.13. In vitro differentiation

All media components used were procured from Life Technologies unless indicated otherwise. For endoderm differentiation, hPSCs were cultured on Matrigel in MEF-conditioned medium supplemented with 30 ng/ml FGF2 until confluency. The medium was then changed to RPMI medium supplemented with 1% (v/v) Gluta-MAX and 100 ng/ml recombinant human Activin A (R&D Systems). Cells were cultured for 3 days, with FBS concentrations at 0% for the first day and 0.2% for the second and third days. Cultures were supplemented with 30 ng/ml purified mouse Wnt3a on the first day.

To initiate ectoderm differentiation, hPSCs were cultured on Matrigel in MEF-conditioned medium supplemented with 30 ng/ml FGF2. Cells were then Accutased for 5 min and re-suspended in neural progenitor cell medium (10% FBS, 1% N2, 1% B27, DMEM/F-12), 5 μM ROCK inhibitor (Y-27632, Stemgent), 50 ng/ml recombinant mouse Noggin (R&D Systems), 0.5 μM dorsomorphin (Tocris Bioscience). Roughly, 7.5×10^5 cells suspended in neural progenitor cell medium were added to each well of several 6-well ultra low attachment plates. The plates were then placed on an orbital shaker at 95 rpm in a 37°C/5% CO_2 incubator for overnight. The formed spherical clusters were then cultured in neural progenitor cell medium supplemented with 50 ng/ml recombinant mouse Noggin and 0.5 μM Dorsomorphin, but no FBS. The medium was subsequently changed every other day. After 5 days in suspension culture, the EBs were then transferred to a 10 cm dish coated (3 × 6 wells per 10 cm dish) with growth factor-reduced Matrigel (1:25 in KnockOut DMEM; BD Biosciences). The cells adhered onto the Matrigel-coated dishes were then cultured in neural progenitor cell medium supplemented with 50 ng/ml recombinant mouse Noggin and 0.5 μM Dorsomorphin. After 7 days of attachment, rosette-forming EBs were collected by manual dissection. Isolated rosettes were incubated in Accutase for 15 minutes in a 37°C, 5% CO_2 tissue culture incubator. The rosettes were then plated onto poly-L-ornithine (PLO; 10 μg/ml; Sigma) and mouse laminin (Ln; 5 μg/ml) coated plates in neural progenitor cell expansion medium [(1% N2, 1% B27, DMEM/F-12) supplemented with 30 ng/ml FGF2 and 30 ng/ml EGF (R & D systems)]. For mesoderm induction, hPSCs were cultured on Matrigel in DMEM supplemented with 20% FBS and 1% penicillin/streptomycin for 21 days.

2.14. Karyotype analysis

To monitor genomic integrity, cells grown on PAm_6-co-PSS_2 hydrogel with StemPro medium or MEF-conditioned medium were evaluated by cytogenetic analysis at passage 16 and 20 using standard protocols for G-banding (Cell Line Genetics).

2.15. PCR array analysis for various extracellular matrix proteins, integrins, and matrix metalloproteinase

Briefly, RNA was isolated from cells using TRIzol (Invitrogen), and treated with DNase I (Invitrogen). Reverse transcription was performed by using RT^2 First Strand Kit (SABioscience, Cat# 330401) and 200 ng of cDNA was processed for quantitative real-time PCR for 84 genes involved in extracellular matrix proteins and adhesion molecules by using PCR array kit (RT^2 Profiler™ PCR Arrays Extracellular matrix and adhesion molecules, PAHS-013A-2, SABioscience) using an ABI Prism 7700 Sequence Detection System (Applied Biosystems). PCR products were quantified by measuring SYBR Green fluorescent dye incorporation with ROX dye reference.

2.16. Protein adsorption

The amount of various proteins adsorbed onto PAm_6-co-$A2AGA_2$ and PAm_6-co-PSS_2 hydrogels was quantified by a modified Bradford protein assay using Bio-Rad Protein Assay kit (Cat# 500-0006) as previously reported (25). Circular hydrogels having 6 mm diameter were prepared and placed onto 96-well plate. These hydrogels were incubated with 200 μl of bovine serum albumin (Sigma, Cat# A8412), vitronectin (Sigma, Cat# V8379-50UG), collagen type I (BD Biosciences, Cat# 354231), collagen type IV (Sigma, Cat# C5533), laminin (Sigma, L6274), and fibronectin (Gibco, Cat# 33016-015) solutions of varying concentrations (0, 2.5, 5, 10, and 15 μg/ml) in PBS for 15 hrs at 4°C. 30 μl of each supernatant solution was mixed with 200 μl of Bradford dye reagent solution, which was prepared according to manufacturer's protocol. 100 μl of the above solution was transferred to a flat-bottom 96-well plate to measure their absorbance at 595 nm by using a Multimode Detector (Beckman Coulter, DTX 880). Three biological replicates were used for the measurements. The adsorption was calculated from a standard curve generated for the corresponding proteins of known concentrations.

2.17. Enzyme-Linked Immunosorbent Assay (ELISA)

The amount of bFGF absorbed by PAm_6-co-$A2AGA_2$ and PAm_6-co-PSS_2 hydrogels was carried out by bFGF ELISA kit (RayBiotech, Inc., cat# ELH-bFGF-001) following the manufacturer's protocol. Similar to the protein absorption assay, circular hydrogels measuring 6 mm in diameter were prepared and placed onto a 96-well plate. These hydrogels were incubated with 250 μl of bFGF (30 ng/mL) at 37°C for approximately 12 hrs. 100 μl of the each supernatant solution was transferred to a bFGF microplate (96 wells coated with anti-human bFGF) and incubated overnight at 4 °C, followed by incubation with a biotinylated antibody and streptavidin solution. After washing, 100 μl of a TMB substrate solution was added to the wells and samples were incubated for 30 mins. Finally, 50 μl of the stop solution was added to samples and their absorbance at 450nm was measured by using a Multimode Detector (Beckman Coulter, DTX 880). Three biological replicates were used for the measurements. The adsorption was calculated from a standard curve generated by bFGF standards provided by the manufacturer.

3. Results

3.1. Design and characterization of synthetic matrices

We synthesized a series of copolymer hydrogels with varying elastic modulus, functional group, and hydrophilicity by copolymerizing acrylamide (Am) with monomers containing either a sulfonate or a carboxylate functional group as described in Supplementary Table S1, Table S2 and Fig. S1. Together, these hydrogels with varying physicochemical properties could provide information on the effect of chemistry, functional group, rigidity, and hydrophilicity of the matrix on supporting self-renewal of hPSCs *in vitro*. The copolymer hydrogels are referred to as PAm_x-co-PB_y, where PAm and PB represent the polymer components of the hydrogel, and x and y denote the mole ratio of the two monomers used in hydrogel synthesis (*see* Supplementary Table S2 for details). For instance, the hydrogels synthesized by copolymerizing acrylamide (Am) and sodium-4-styrenesulfonate (SS) at a mole ratio of 6:2 is denoted as PAm_6-co-PSS_2. Figure 1a shows the schematic of the synthetic matrices containing PAm and PSS moieties (e.g. PAm_x-co-PSS_y). The elastic modulus and hydrophilicity of these hydrogels are listed in Supplementary Table S2. For example, the PAm_6-co-PSS_2 hydrogels exhibited an elastic modulus of 343.7 ± 5.1 kPa, and a hydrophilicity of 23.0 ± 2.0°.

3.2. PSS-based hydrogels support self-renewal and long-term expansion of hPSCs

Our initial observation was that the HUES9 cells cultured on PAm_6-co-PSS_2 hydrogels adhered onto the underlying hydrogel and formed bright and compact colonies. However, differences in cell adhesion were observed between PAm_6-co-PSS_2 hydrogels and their control counterparts— MEF- and Matrigel- supported cultures. Observations after 24 hrs of cell seeding indicated that the number of cells adhered onto both MEF and Matrigel are significantly higher compared to PAm_6-co-PSS_2 hydrogels. Despite these differences, the cells adhered onto PAm_6-co-PSS_2 hydrogels, proliferated and formed compact colonies similar to those observed on Matrigel- and MEF-supported cultures (Fig. 1b–d). The population doubling time of HUES9 cells on PAm_6-co-PSS_2 hydrogels was found to be ~38 hrs, while that on MEFs and Matrigel was found to be ~23 hrs (Fig. 1e). The estimated population doubling time on PAm_6-co-PSS_2 hydrogels is likely an overestimate given that the cell-cell adhesion of cells grown on these hydrogels were significantly higher compared to those on Matrigel- and MEF-supported cultures; strong cell-cell adhesion limits the uniform dissociation of hESC colonies into single cells.

Although the aforementioned findings show that HUES9 cells can adhere and grow on PAm_6-co-PSS_2 hydrogels, it is vital to test whether the developed matrix can support the long-term expansion of hPSCs without compromising their pluripotency and karyotypic stability. The PAm_6-co-PSS_2 hydrogels indeed supported adhesion and long-term growth of HUES9 cells both in MEF-conditioned medium and chemically defined StemPro medium (Supplementary Fig. S2a, Fig. 2). HUES9 cells expanded on PAm_6-co-PSS_2 hydrogels with frequent splitting for over 20 passages (> 8 months) using StemPro medium exhibited characteristic stem cell morphology and tight colony formation (Fig. 2a). The expanded HUES9 cells were positive for OCT4 and NANOG. The real-time PCR (qPCR) results indicate that hPSCs exhibited similar gene expression levels of OCT4 and NANOG

compared to those cultured on Matrigel (Fig. 2b). The pluripotency of HUES9 cells expanded on PAm_6-co-PSS_2 hydrogels was further confirmed by FACS analysis, which revealed a similar percentage of pluripotent cells between those cultured on PAm_6-co-PSS_2 and Matrigel, as evidenced by the population of OCT4 and TRA1-81 positive cells (Fig. 2c).

One of the unique characteristics of pluripotent stem cells is their ability to form embryoid bodies (EBs) in suspension culture and differentiate into all three germ layers. The HUES9 cells grown on PAm_6-co-PSS_2 hydrogels formed EBs (Supplementary Fig. S3). The cells expanded on PAm_6-co-PSS_2 matrices were also differentiated into mesoderm, ectoderm, and endoderm, further confirming that the cells grown extensively on these hydrogels maintained their ability to differentiate into multiple germ layers (Fig. 3a,b). Additionally, the cells cultured on PAm_6-co-PSS_2 maintained a normal karyotype (Fig. 3c and Supplementary Fig. S2b). Together, these findings demonstrate the potential of PAm_6-co-PSS_2 to support long-term culture of undifferentiated hPSCs while maintaining their pluripotency.

To determine whether the PAm_6-co-PSS_2-assisted self-renewal of HUES9 cells is applicable to other hPSCs, we have investigated the potential of PAm_6-co-PSS_2 to support the growth of HUES6 and human induced pluripotent stem cells (hiPSCs) *in vitro*. Similar to HUES9 cells, HUES6 and hiPSCs cultured and passaged over multiple times on PAm_6-co-PSS_2 hydrogels in StemPro medium displayed characteristic hPSC morphology, bright colony formation, and OCT4 and NANOG expression comparable to Matrigel (Fig. 4a,b and Supplementary Fig. S4a,b).

3.3. Effect of matrix rigidity on hPSCs

Having established the unique ability of PAm_6-co-PSS_2 hydrogels containing PSS moieties to support the growth of hPSCs *in vitro* while maintaining their pluripotency, we next determined the effect of matrix rigidity on hPSCs. To this end, we synthesized PAm_6-co-PSS_2 hydrogels with different bulk moduli (~54, ~138, and ~344 kPa) by varying their cross-link density (*see* Supplementary Table S2). Note that the changes in modulus also introduce subtle changes in matrix hydrophilicity as rigidity affects swelling, which in turn affects the surface density of sulfonate functional groups accessible at the interface. As seen from Fig. 5a, an increased cell adhesion and colony formation was observed with increasing rigidity of PAm_6-co-PSS_2 hydrogels. Hydrogels having a compressive modulus of ~344 kPa supported adhesion, colony formation, and pluripotency of HUES9-Oct4-GFP cells. Supplementary Fig. S5 demonstrates the growth of HUES9 cells on these PAm_6-co-PSS_2 hydrogels having higher elastic modulus (~344 kPa). PAm_6-co-PSS_2 hydrogels with low bulk rigidity (~54 kPa) supported minimal cell adhesion while those having a rigidity of ~138 kPa exhibited moderate cell adhesion, but the attached cells underwent spontaneous differentiation.

3.4. Effects of chemical functional group(s) and matrix hydrophilicity on hPSCs

We next investigated the effect of hydrogel composition on adhesion and growth of hPSCs by varying the amount of PSS content within the hydrogels (mole ratio of Am:SS 6:0.5, 6:1, 6:2). Significant differences in adhesion and colony formation of HUES9-Oct4-GFP cells

were observed amongst the hydrogels; specifically a monotonic dependence with the PSS content was observed (Fig. 5b, Supplementary Fig. S6a). No cell adhesion was observed on hydrogels containing lower amounts of PSS moieties (PAm_6-co-$PSS_{0.5}$). While an increase in PSS content in the hydrogel (PAm_6-co-PSS_1) supported cell adhesion, they failed to support the colony formation of adhered cells. A further increase in PSS content, as in PAm_6-co-PSS_2, supported both adhesion and colony formation of HUES9-Oct4-GFP cells (Fig. 5b, Supplementary Fig. S6a). Note that varying the hydrogel composition also introduced subtle changes to their hydrophilicity and bulk rigidity (Supplementary Table S2).

Given the importance of functional group and matrix hydrophilicity on cell adhesion, we also evaluated cellular responses of HUES9 cells on different hydrogels with varying hydrophilicity. These hydrogels were created by reacting Am with different monomers (SS, SPA and MEDSAH) terminating with sulfonate functional group at a mole ratio of 6:2 (Am:comonomer). These hydrogels have similar elastic moduli and functional groups but varying matrix hydrophilicities (Supplementary Table S2). Similar to PAm_6-co-PSS_2 hydrogels, significant cell adhesion was observed initially on PAm_6-co-$PSPA_2$ hydrogels, while minimal to no cell adhesion was observed on PAm_6-co-$PMEDSAH_2$ (Fig. 5c). However, unlike PAm_6-co-PSS_2 hydrogels, cells on PAm_6-co-$PSPA_2$ did not grow to form bright compact colonies (Fig. 5c).

These results clearly indicate the effect of multiple physical and chemical cues of the underlying matrix on hPSC response. In an effort to delineate the effect of various material properties from that of the functional group, we synthesized copolymer hydrogels bearing carboxylate groups (PAm_6-co-$PA2AGA_2$) having similar elastic modulus, hydrophilicity, and topography to that of PAm_6-co-PSS_2 (Supplementary Table S2 and Fig. S7). Unlike PAm_6-co-PSS_2, the HUES9 cells on PAm_6-co-$PA2AGA_2$ hydrogels exhibited minimal to no cell adhesion (Supplementary Fig. S6b,c). We also examined the effect of carboxyl functional groups on hPSCs by employing different PAm_6-co-PB_2 hydrogels having carboxyl functional groups but varying hydrophilicity (Supplementary Table S2) (23). Similar to PAm_6-co-$PA2AGA_2$, no cell adhesion was observed on hydrogels with carboxyl functional groups (data not shown). These findings demonstrate the importance of sulfonate groups on the observed PAm_6-co-PSS_2- mediated cell response.

3.5. Cell-matrix interface on adhesion and growth of hPSCs

As the interface of the hydrogels was not functionalized with proteins or peptides and a short incubation of the hydrogels in serum medium prior to cell seeding was needed for initial cell adhesion, we examined the adsorption of various extracellular matrix proteins (ECM) onto the hydrogel surfaces. It is well known that matrix interfacial properties (hydrophilicity, functional group, surface roughness, rigidity, etc.) affect protein adsorption and conformation, thereby influencing cell adhesion (23, 26, 27). We examined protein adsorption on PAm6-co-PSS2 hydrogels and compared it to PAm_6-co-$PA2AGA_2$. We chose these two hydrogels based on our observation that despite having similar hydrophilicity, surface roughness, and rigidity, PAm_6-co-PSS_2 hydrogels support hPSCs while PAm_6-co-$PA2AGA_2$ hydrogels do not. We also examined the adsorption of bFGF on either hydrogel.

While both the hydrogels supported adsorption of ECM proteins and bFGF, PAm_6-co-PSS_2 hydrogels was found to adsorb slightly higher amounts of certain proteins such as BSA and VN compared to PAm_6-co-$PA2AGA_2$ (Fig. 6a,b).

Cell surface adhesion molecules such as integrins play an important role in the adhesion of hPSCs to the underlying ECM, and also in the regulation of their self-renewal (28–30). Similarly, ECM components secreted by the hPSCs and the feeder cells have also been shown to play an important role in maintaining the pluripotency of hPSCs (18, 31). To this end, we determined the endogenous expressions levels of various cell surface adhesion molecules and ECM components of HUES9 cells cultured on PAm_6-co-PSS_2 and PAm_6-co-$PSPA_2$, and compared the results against those of MEF- and Matrigel-supported culture under identical conditions. The PAm_6-co-$PSPA_2$ hydrogel was chosen as it supported initial adhesion of HUES9 cells similar to PAm_6-co-PSS_2, but failed to support their growth and colony formation. As seen from Fig. 6c, the underlying matrix had a significant effect on the gene expression profile of the cells. In short, the cells on PAm_6-co-PSS_2 hydrogels exhibited higher expression levels of various integrins and ECM proteins that are known to be relevant to self-renewal of hPSCs. Specifically, HUES9 cells cultured on PAm_6-co-PSS_2 expressed higher levels of fibronectin, laminin, collagen, and vitronectin, as well as integrins α_1, α_2, α_8, and α_V. Many of these ECM proteins and integrins have been implicated to play an important role in self-renewal of hPSCs (10, 11, 28, 30, 32). Additionally, cells on PAm_6-co-PSS_2 hydrogels expressed higher levels of MMP family of proteins indicating the potential role of ECM remodeling.

4. Discussion

HPSCs such as hESCs and iPSCs grow best when cultured on feeder cells such as MEFs or Matrigel (33, 34). Emerging evidence shows that biomaterial-based matrices can also support *in vitro* expansion of hPSCs without compromising their phenotypic and differentiation potential (8, 10, 14, 15). In this study, we demonstrate the potential of synthetic hydrogels containing heparin-mimicking PSS moieties in supporting the *in vitro* growth and self-renewal of hPSCs. The synthetic matrix, PAm_6-co-PSS_2, supported the growth and expansion of multiple hPSC lines (HUES9, HUES6, and hiPSCs) through multiple passages (≥20 passages) while maintaining their pluripotency.

Our results indicate that the presence of sulfonate groups alone is not sufficient to support self-renewal of hPSCs, but a combination of physical cues such as hydrophilicity and elastic modulus is required, thus exemplifying the delicate balance of insoluble and soluble cues of the niche on various cellular responses of hPSCs. Previous studies by Villa-Diaz et al. have shown that PMEDSAH-coated dishes having a water contact angle of ~17° supported self-renewal of hESCs in StemPro medium(8). However, PAm_6-co-$PMEDSAH_2$ hydrogels failed to support hPSCs adhesion and growth; this could be attributed to the differences in chemical composition and/or the hydrophilicity of the matrix. Indeed, functional groups and hydrophilicity have been shown to play a key role in modulating the adsorption and conformation of proteins, and the sequestration of growth factors(10, 23, 35). These subtle changes of the cell-matrix interface can have a significant effect on mediating the initial adhesion of hPSCs onto the matrix(25).

Despite having the same hydrophilicity, elastic modulus, and surface roughness, PAm_6-co-PSS_2 and PAm_6-co-$PA2AGA_2$ hydrogels elicited different cellular responses. These differences in cellular responses could be attributed to changes in ECM proteins that are adsorbed onto the hydrogel interface, with significant alterations in the extent of BSA and VN adsorbed between the surfaces. Previous studies have shown that the adsorption of BSA and VN onto hydrogel surfaces can foster adhesion and self-renewal of hPSCs(10, 15). It is also possible that besides the amount of proteins at the interface, the conformation of proteins plays a role in mediating cell adhesion (36–40). Another possibility is the differences in matrix-bFGF binding strength, which could lead to changes in bFGF signaling(35).

Together, our results suggest that the adhesive interface of the PAm_6-co-PSS_2 matrices, mediated through protein adsorption, supports initial adhesion of hPSCs, which in turn facilitate both cell-matrix and cell-cell interactions to allow colony formation of the adhered cells. While the adsorbed proteins support initial adhesion of seeded cells, it is likely that the cell-secreted ECM proteins are the ones that support long-term maintenance and growth of these cells, as shown by the transcription profile. The reciprocal interactions of cells with their surrounding ECM play an important role in their fate determination as ECM components can induce various intracellular signals to drive self-renewal vs. differentiation decisions. Recent studies have indicated the importance of a combination of integrins and ECM proteins in maintaining stemness of pluripotent cells(28, 30). For instance, a recent study by Meng et al., demonstrated the superior effect of matrices comprising of several peptides over that of single peptide on supporting self-renewal of hESCs(30). A similar finding was also reported by Brafman et al., which showed the beneficial effect of a combination of ECM proteins on supporting self-renewal of hESCs(17). In addition to ECM proteins and integrins, the cells cultured on PAm_6-co-PSS_2 hydrogels exhibit higher levels of MMP proteins indicating potential ECM remodeling in hPSC self-renewal. This result is consistent with a recent study, which demonstrated the role of ECM remodeling and endogenous cell-secreted factors on self-renewal of mouse embryonic stem cells (mESCs) (31). Any perturbations to the ESC-secreted signaling resulted in the mESCs exiting their self-renewal state, thus demonstrating the importance of autocrine factors on self-renewal of pluripotent stem cells.

In conclusion, this study demonstrates that synthetic hydrogels having a combination of physicochemical properties support adhesion and growth of hPSCs by activating cellular processes and harnessing autocrine factors that are conducive for self-renewal of hPSCs. The hydrogel-based synthetic matrices introduced here support adhesion of hPSCs and their long-term growth without compromising their pluripotency and karyotypic stability. Such tunable synthetic matrices also serve as platforms to elucidate the roles of different biophysical and biochemical cues in cell-matrix and cell-cell interactions.

Supplementary Material

Refer to Web version on PubMed Central for supplementary material.

Acknowledgments

We acknowledge Profs. S. Chien and G. Arya for valuable discussions. We also thank the financial support from California Institute of Regenerative Medicine (RN2-00945 and RT2-01889).

References

1. Ludwig TE, Levenstein ME, Jones JM, Berggren WT, Mitchen ER, Frane JL, et al. Derivation of human embryonic stem cells in defined conditions. Nat Biotechnol. 2006; 24(2):185–187. [PubMed: 16388305]
2. Hwang Y, Phadke A, Varghese S. Engineered microenvironments for self-renewal and musculoskeletal differentiation of stem cells. Regen Med. 2011; 6(4):505–524. [PubMed: 21749208]
3. Amit M, Shariki C, Margulets V, Itskovitz-Eldor J. Feeder layer- and serum-free culture of human embryonic stem cells. Biol Reprod. 2004; 70(3):837–845. [PubMed: 14627547]
4. Furue MK, Na J, Jackson JP, Okamoto T, Jones M, Baker D, et al. Heparin promotes the growth of human embryonic stem cells in a defined serum-free medium. Proc Natl Acad Sci U S A. 2008; 105(36):13409–13414. [PubMed: 18725626]
5. Bergstrom R, Strom S, Holm F, Feki A, Hovatta O. Xeno-free culture of human pluripotent stem cells. Methods Mol Biol. 2011; 767:125–136. [PubMed: 21822871]
6. Richards M, Fong CY, Chan WK, Wong PC, Bongso A. Human feeders support prolonged undifferentiated growth of human inner cell masses and embryonic stem cells. Nat Biotechnol. 2002; 20(9):933–936. [PubMed: 12161760]
7. Melkoumian Z, Weber JL, Weber DM, Fadeev AG, Zhou Y, Dolley-Sonneville P, et al. Synthetic peptide-acrylate surfaces for long-term self-renewal and cardiomyocyte differentiation of human embryonic stem cells. Nat Biotechnol. 2010; 28(6):606–610. [PubMed: 20512120]
8. Villa-Diaz LG, Nandivada H, Ding J, Nogueira-de-Souza NC, Krebsbach PH, O'Shea KS, et al. Synthetic polymer coatings for long-term growth of human embryonic stem cells. Nat Biotechnol. 2010; 28(6):581–583. [PubMed: 20512122]
9. Derda R, Musah S, Orner BP, Klim JR, Li L, Kiessling LL. High-throughput discovery of synthetic surfaces that support proliferation of pluripotent cells. J Am Chem Soc. 2010; 132(4):1289–1295. [PubMed: 20067240]
10. Mei Y, Saha K, Bogatyrev SR, Yang J, Hook AL, Kalcioglu ZI, et al. Combinatorial development of biomaterials for clonal growth of human pluripotent stem cells. Nat Mater. 2010; 9(9):768–778. [PubMed: 20729850]
11. Rodin S, Domogatskaya A, Strom S, Hansson EM, Chien KR, Inzunza J, et al. Long-term self-renewal of human pluripotent stem cells on human recombinant laminin-511. Nat Biotechnol. 2010; 28(6):611–615. [PubMed: 20512123]
12. Klim JR, Li L, Wrighton PJ, Piekarczyk MS, Kiessling LL. A defined glycosaminoglycanbinding substratum for human pluripotent stem cells. Nat Methods. 2010; 7(12):989–994. [PubMed: 21076418]
13. Kolhar P, Kotamraju VR, Hikita ST, Clegg DO, Ruoslahti E. Synthetic surfaces for human embryonic stem cell culture. J Biotechnol. 2010; 146(3):143–146. [PubMed: 20132848]
14. Brafman DA, Chang CW, Fernandez A, Willert K, Varghese S, Chien S. Long-term human pluripotent stem cell self-renewal on synthetic polymer surfaces. Biomaterials. 2010; 31(34): 9135–9144. [PubMed: 20817292]
15. Irwin EF, Gupta R, Dashti DC, Healy KE. Engineered polymer-media interfaces for the long-term self-renewal of human embryonic stem cells. Biomaterials. 2011; 32(29):6912–6919. [PubMed: 21774983]
16. Saha K, Mei Y, Reisterer CM, Pyzocha NK, Yang J, Muffat J, et al. Surface-engineered substrates for improved human pluripotent stem cell culture under fully defined conditions. Proc Natl Acad Sci U S A. 2011; 108(46):18714–18719. [PubMed: 22065768]

17. Brafman DA, Shah KD, Fellner T, Chien S, Willert K. Defining long-term maintenance conditions of human embryonic stem cells with arrayed cellular microenvironment technology. Stem Cells Dev. 2009; 18(8):1141–1154. [PubMed: 19327010]
18. Levenstein ME, Berggren WT, Lee JE, Conard KR, Llanas RA, Wagner RJ, et al. Secreted proteoglycans directly mediate human embryonic stem cell-basic fibroblast growth factor 2 interactions critical for proliferation. Stem Cells. 2008; 26(12):3099–3107. [PubMed: 18802039]
19. Sangaj N, Kyriakakis P, Yang D, Chang CW, Arya G, Varghese S. Heparin mimicking polymer promotes myogenic differentiation of muscle progenitor cells. Biomacromolecules. 2010; 11(12): 3294–3300. [PubMed: 21058638]
20. Shimokawa K, Kimura-Yoshida C, Nagai N, Mukai K, Matsubara K, Watanabe H, et al. Cell surface heparan sulfate chains regulate local reception of FGF signaling in the mouse embryo. Dev Cell. 2011; 21(2):257–272. [PubMed: 21839920]
21. Spivak-Kroizman T, Lemmon MA, Dikic I, Ladbury JE, Pinchasi D, Huang J, et al. Heparin-induced oligomerization of FGF molecules is responsible for FGF receptor dimerization, activation, and cell proliferation. Cell. 1994; 79(6):1015–1024. [PubMed: 7528103]
22. Vlodavsky I, Miao HQ, Medalion B, Danagher P, Ron D. Involvement of heparan sulfate and related molecules in sequestration and growth promoting activity of fibroblast growth factor. Cancer Metastasis Rev. 1996; 15(2):177–186. [PubMed: 8842489]
23. Ayala R, Zhang C, Yang D, Hwang Y, Aung A, Shroff SS, et al. Engineering the cell-material interface for controlling stem cell adhesion, migration, and differentiation. Biomaterials. 2011; 32(15):3700–3711. [PubMed: 21396708]
24. Zhang C, Aung A, Liao LQ, Varghese S. A novel single precursor-based biodegradable hydrogel with enhanced mechanical properties. Soft Matter. 2009; 5(20):3831–3834.
25. Yap LY, Li J, Phang IY, Ong LT, Ow JZ, Goh JC, et al. Defining a threshold surface density of vitronectin for the stable expansion of human embryonic stem cells. Tissue Eng Part C Methods. 2011; 17(2):193–207. [PubMed: 20726687]
26. Llopis-Hernandez V, Rico P, Ballester-Beltran J, Moratal D, Salmeron-Sanchez M. Role of surface chemistry in protein remodeling at the cell-material interface. PLoS One. 2011; 6(5):e19610. [PubMed: 21573010]
27. Trappmann B, Gautrot JE, Connelly JT, Strange DG, Li Y, Oyen ML, et al. Extracellular-matrix tethering regulates stem-cell fate. Nat Mater. 2012; 11:642–649. [PubMed: 22635042]
28. Lee ST, Yun JI, Jo YS, Mochizuki M, van der Vlies AJ, Kontos S, et al. Engineering integrin signaling for promoting embryonic stem cell self-renewal in a precisely defined niche. Biomaterials. 2010; 31(6):1219–1226. [PubMed: 19926127]
29. Hayashi Y, Furue MK, Okamoto T, Ohnuma K, Myoishi Y, Fukuhara Y, et al. Integrins regulate mouse embryonic stem cell self-renewal. Stem Cells. 2007; 25(12):3005–3015. [PubMed: 17717067]
30. Meng Y, Eshghi S, Li YJ, Schmidt R, Schaffer DV, Healy KE. Characterization of integrin engagement during defined human embryonic stem cell culture. Faseb J. 2010; 24(4):1056–1065. [PubMed: 19933311]
31. Przybyla LM, Voldman J. Attenuation of extrinsic signaling reveals the importance of matrix remodeling on maintenance of embryonic stem cell self-renewal. Proc Natl Acad Sci U S A. 2012; 109(3):835–840. [PubMed: 22215601]
32. Braam SR, Zeinstra L, Litjens S, Ward-van Oostwaard D, van den Brink S, van Laake L, et al. Recombinant vitronectin is a functionally defined substrate that supports human embryonic stem cell self-renewal via alphavbeta5 integrin. Stem Cells. 2008; 26(9):2257–2265. [PubMed: 18599809]
33. Thomson JA, Itskovitz-Eldor J, Shapiro SS, Waknitz MA, Swiergiel JJ, Marshall VS, et al. Embryonic stem cell lines derived from human blastocysts. Science. 1998; 282(5391):1145–1147. [PubMed: 9804556]
34. Xu C, Inokuma MS, Denham J, Golds K, Kundu P, Gold JD, et al. Feeder-free growth of undifferentiated human embryonic stem cells. Nat Biotechnol. 2001; 19(10):971–974. [PubMed: 11581665]

35. Hudalla GA, Koepsel JT, Murphy WL. Surfaces that sequester serum-borne heparin amplify growth factor activity. Adv Mater. 2011; 23(45):5415–5418. [PubMed: 22028244]

36. Michael KE, Vernekar VN, Keselowsky BG, Meredith JC, Latour RA, Garcia AJ. Adsorption-induced conformational changes in fibronectin due to interactions with well-defined surface chemistries. Langmuir. 2003; 19(19):8033–8040.

37. Grinnell F, Feld MK. Fibronectin Adsorption on Hydrophilic and Hydrophobic Surfaces Detected by Antibody-Binding and Analyzed during Cell-Adhesion in Serum-Containing Medium. J Biol Chem. 1982; 257(9):4888–4893. [PubMed: 7068668]

38. Tengvall P, Lundstrom I, Liedberg B. Protein adsorption studies on model organic surfaces: an ellipsometric and infrared spectroscopic approach. Biomaterials. 1998; 19(4–5):407–422. [PubMed: 9677154]

39. Iuliano DJ, Saavedra SS, Truskey GA. Effect of the Conformation and Orientation of Adsorbed Fibronectin on Endothelial-Cell Spreading and the Strength of Adhesion. J Biomed Mater Res. 1993; 27(8):1103–1113. [PubMed: 8408123]

40. Pettit DK, Hoffman AS, Horbett TA. Correlation between Corneal Epithelial-Cell Outgrowth and Monoclonal-Antibody Binding to the Cell-Binding Domain of Adsorbed Fibronectin. J Biomed Mater Res. 1994; 28(6):685–691. [PubMed: 8071379]

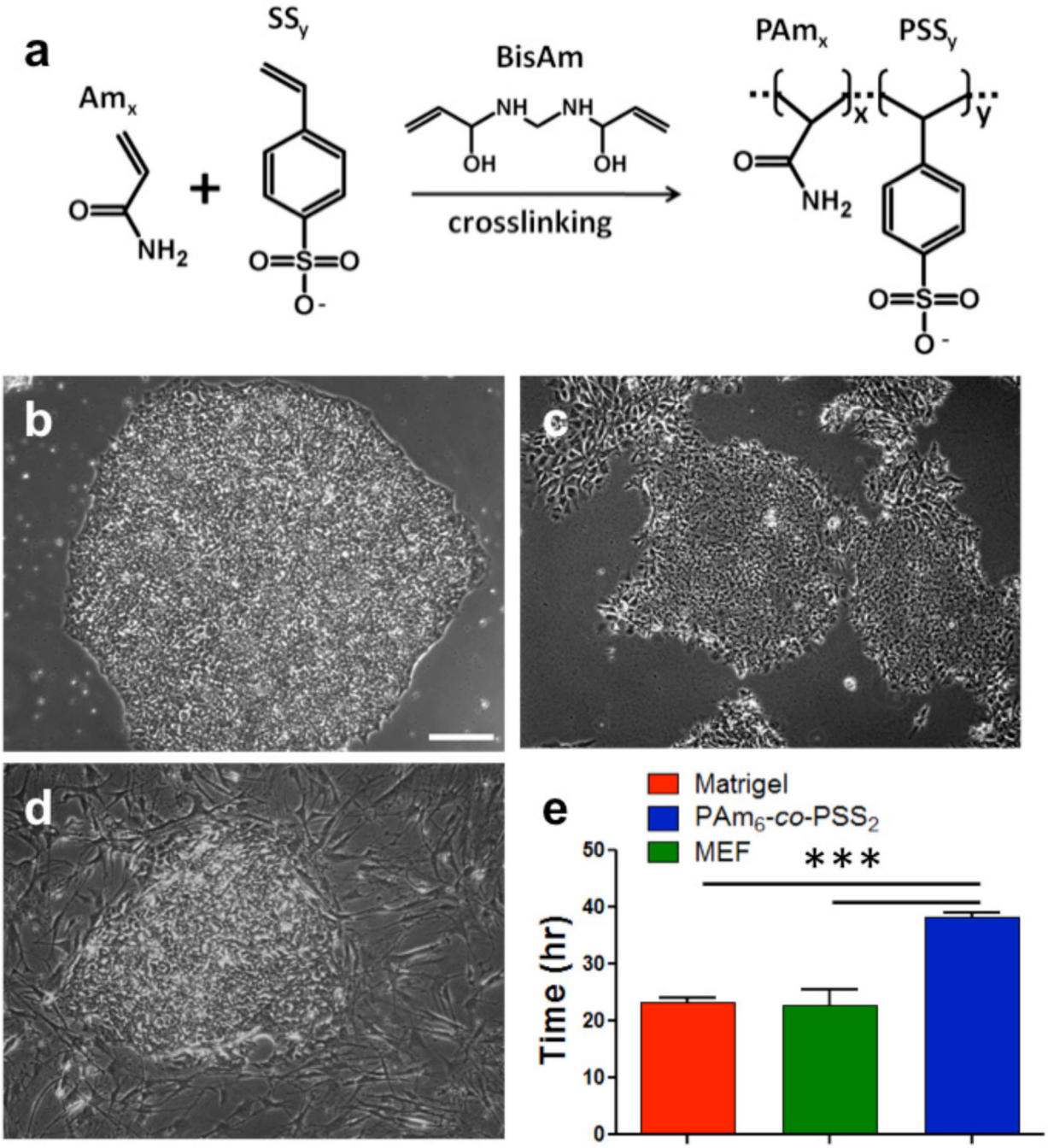

Figure 1.

PSS-based hydrogels support growth of HUES9 cells *in vitro*. (a) Schematic of PSS-based hydrogel(s) synthesized by copolymerizing acrylamide with sodium 4-vinyl benzene sulfonate with bisacrylamide as a crosslinking agent. Representative phase contrast images of HUES9 colonies on (b) PAm_6-co-PSS_2 hydrogel, (c) Matrigel, and (d) mouse embryonic fibroblasts (MEFs) after 7 days in culture in StemPro medium. (e) Population doubling of HUES9 cells over five days of B–D. Scale bar: 200μm. Values are shows as mean ± SD. *** $p < 0.001$.

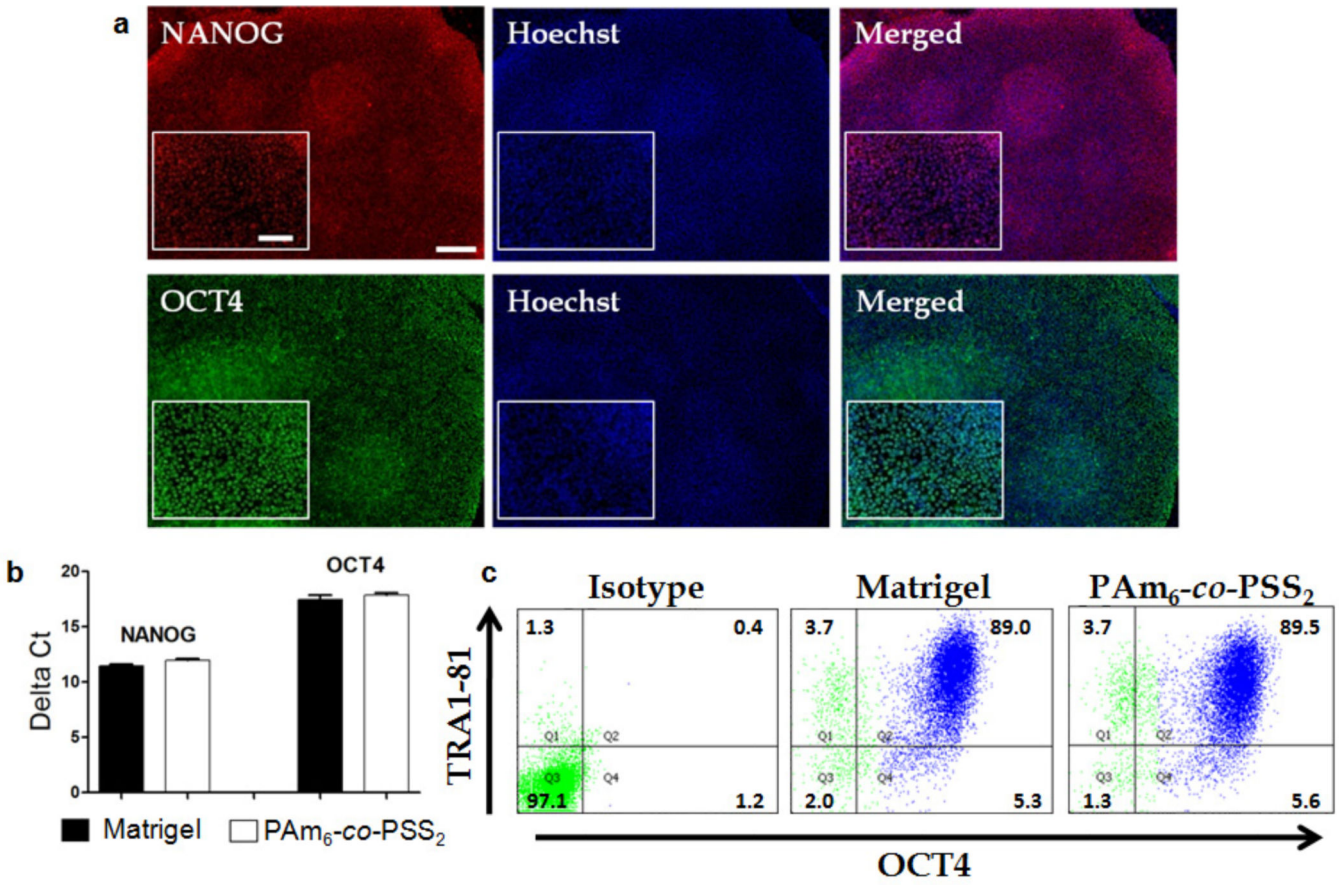

Figure 2.

PSS-based synthetic matrices supported long-term maintenance of HUES9 in StemPro medium. (a) HUES9 cells grown on PAm_6-co-PSS_2 hydrogels in StemPro medium for 20 passages stained positive for NANOG (Red) and OCT4 (Green). The nuclei are stained blue with Hoescht 33342. The inset shows higher magnification images. Scale bar: 200μm (main images) and 100μm (inset images). (b) Quantitative PCR of HUES9 cells grown on PAm_6-co-PSS_2 hydrogels showed similar expression level of OCT4 and NANOG to that on Matrigel. (c) Representative FACS profiles of HUES9 cells grown on PAm_6-co-PSS_2 hydrogel and Matrigel, which again shows PAm_6-co-PSS_2 hydrogels can support *in vitro* self-renewal of HUES9 cells similar to Matrigel.

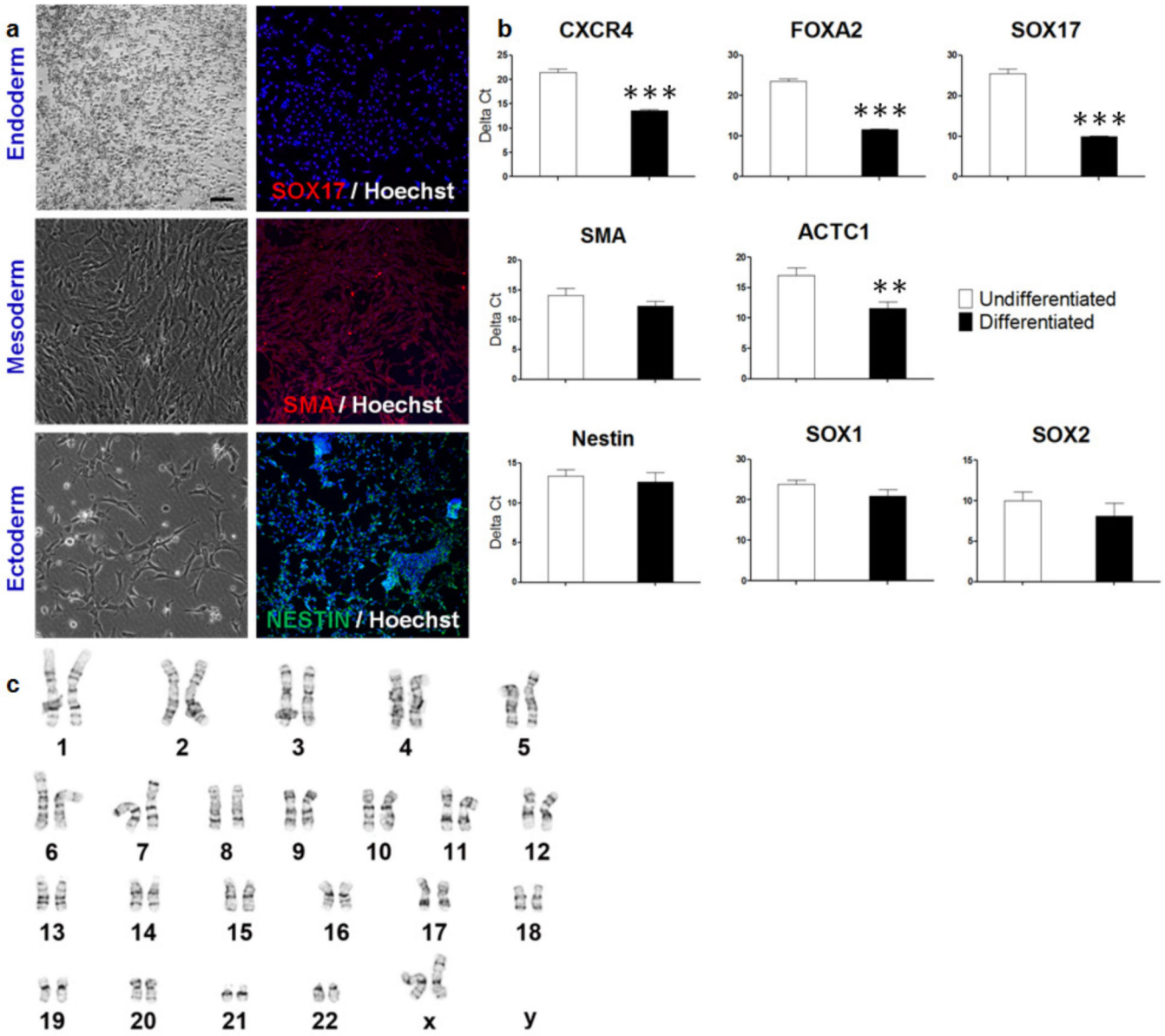

Figure 3.

In vitro differentiation of HUES9 cells passaged 20 times using PAm_6-co-PSS_2 hydrogels. (a) Immunofluorescence staining shows differentiation of these cells into endoderm (SOX17), mesoderm (SMA), and ectoderm (Nestin) lineages. Scale bar = 100μm. (b) Quantitative PCR results for differentiated HUES9 cells shows expression of ectoderm (CXCR4, FOXA2, SOX17), mesoderm (SMA, ACTC1), and ectoderm markers (Nestin, SOX1, SOX2). (c) Karyotype analysis of HUES9 cells grown on PAm_6-co-PSS_2 hydrogel shows a normal euploid karyotype. Values are shown as mean ± SD. ** $p < 0.01$ and *** $p < 0.001$.

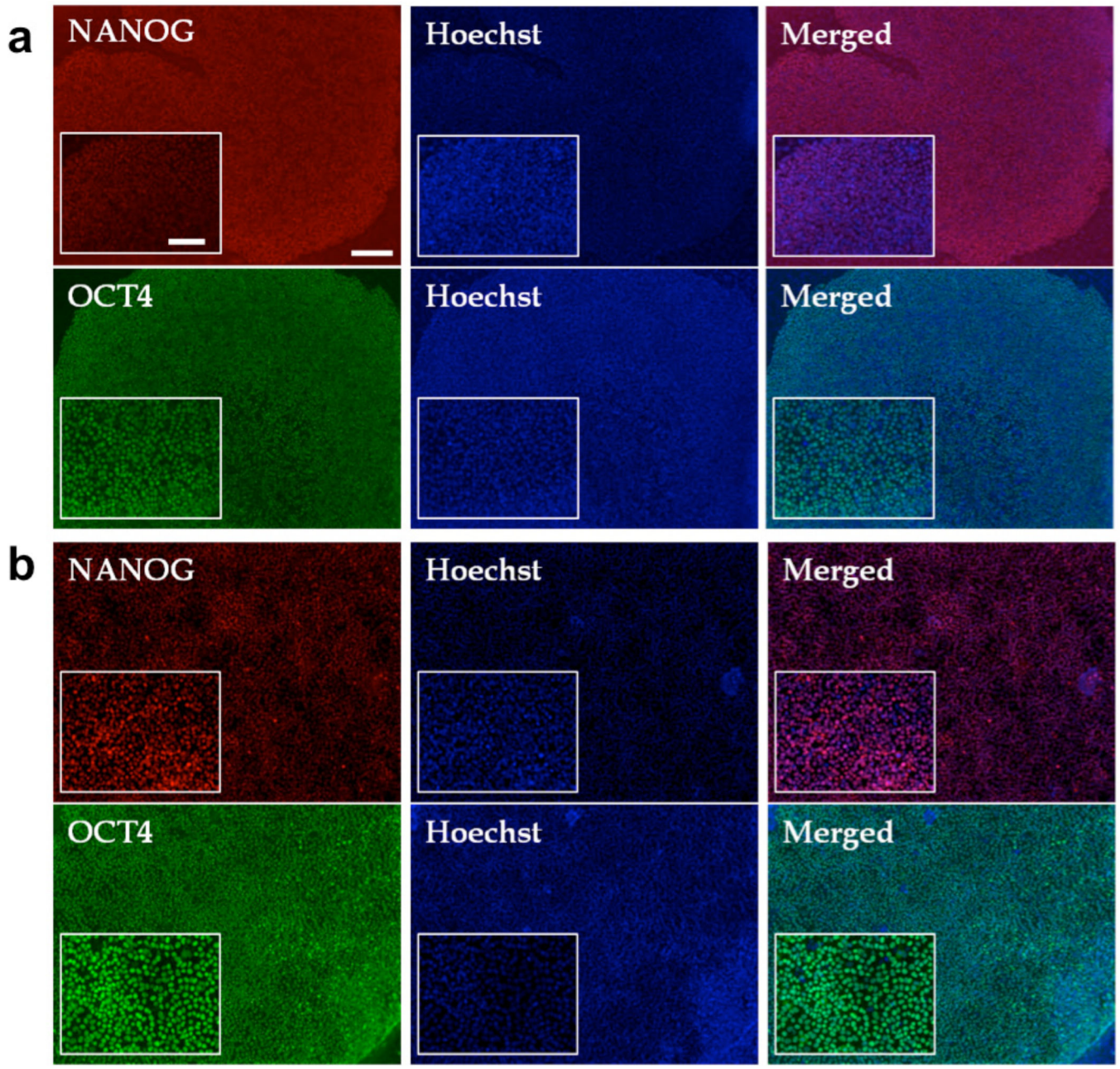

Figure 4.

PAm_6-co-PSS_2 hydrogel supported *in vitro* growth of HUES6 and human induced pluripotent stem cells (hiPSCs) grown over multiple passages in StemPro medium. Immunofluorescence staining of (a) HUES6 and (b) hiPSCs after passages 7 and 9, respectively. Red for NANOG and Green for OCT4, while nuclei are stained blue with Hoescht 33342. Scale bar: 200μm (main images) and 100μm (inset images).

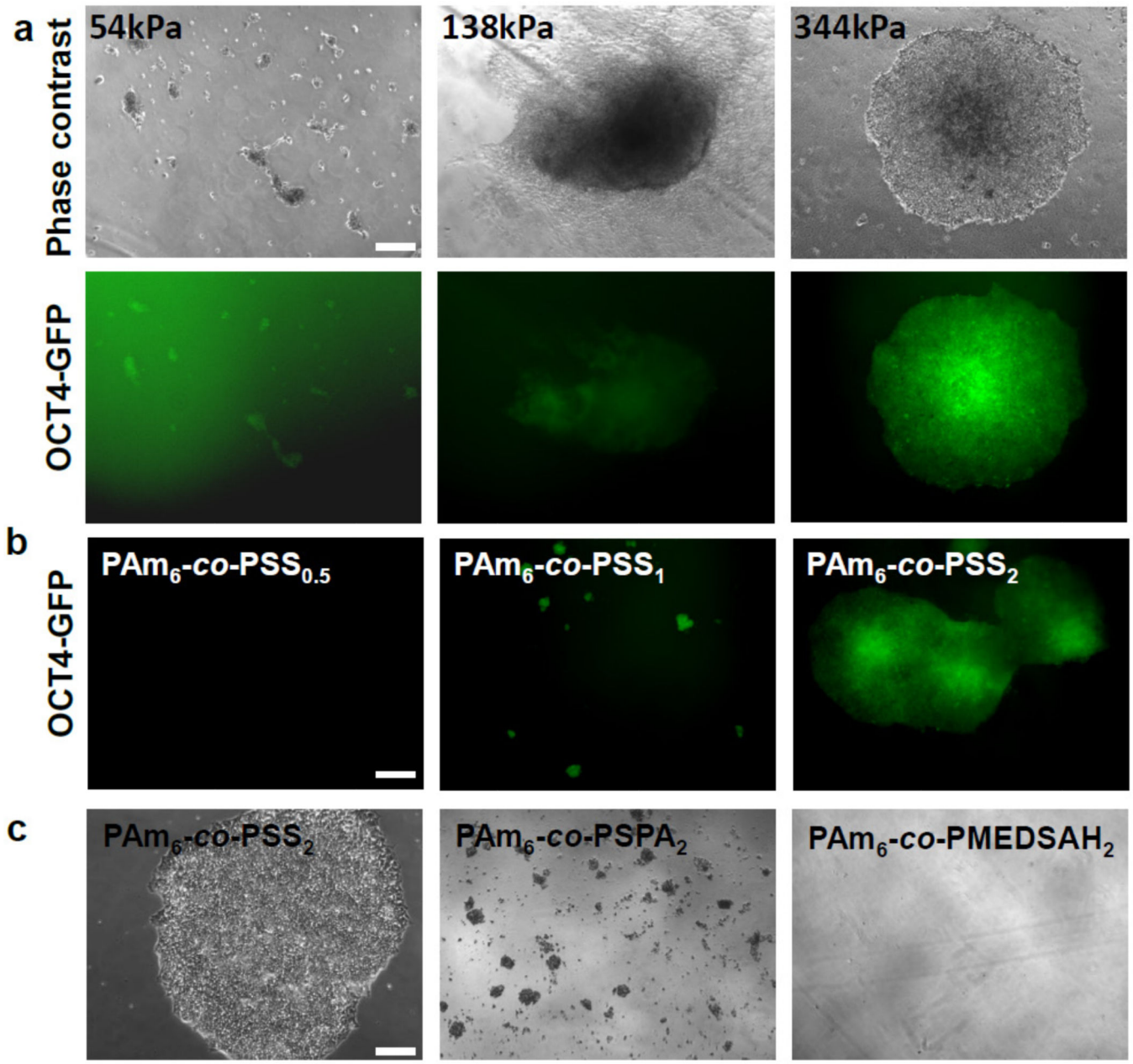

Figure 5.

Effect of matrix rigidity, chemistry, and hydrophilicity on hPSCs. (a) Representative phase contrast images of adhered HUES9-Oct4-GFP cells on PSS-based hydrogels with varying bulk rigidity (top) and their corresponding fluorescence images (bottom). (b) Images of HUES9-Oct4-GFP cells on PSS-based hydrogels with varying mole ratio of acrylamide to sodium 4-vinyl benzene sulfonate (Am:SS; 6:0.5, 6:1, and 6:2); PAm_6-co-$PSS_{0.5}$, PAm_6-co-PSS_1, PAm_6-co-PSS_2 (top) (c) Representative phase contrast images of hPSCs grown on hydrogels containing different chemistries and hydrophilicities while maintaining identical sulfate functional groups and matrix rigidities. Scale bar: 200μm.

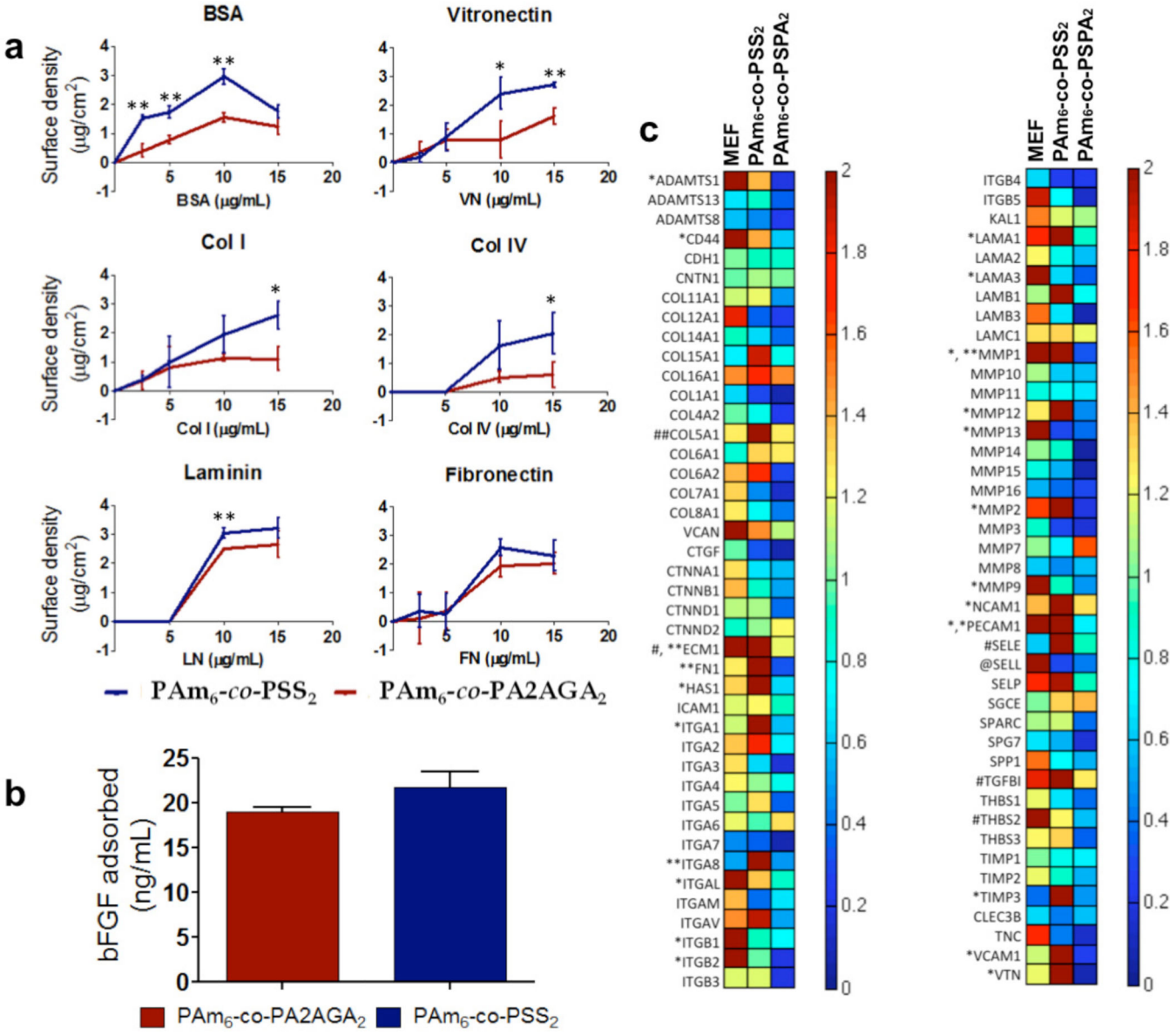

Figure 6.

Characterization of cell-material interface. (a) Quantification of various extracellular matrix proteins adsorbed onto PAm_6-co-PSS_2 hydrogel (blue) and PAm_6-co $PA2AGA_2$ hydrogel (red). BSA; bovine serum albumin, VN; vitronectin, Col1; collagen type I, Col4; collagen type IV, LN; laminin, FN; fibronectin. (b) bFGF adsorption onto PAm_6-co-PSS_2 (blue) and PAm_6-co-$PA2AGA_2$ (red) hydrogel(s). Values are shown as mean ± SD. *$p < 0.05$ and ** $p < 0.01$, (c) Hierarchical cluster analysis of transcription profile of HUES9 cells cultured on MEFs, PAm_6-co-PSS_2, and PAm_6-co-$PSPA_2$. Expression levels are normalized to that of Matrigel. The notations *, **, #, and ## indicates 2–5 times, 5–10 times, 10–15 times, and >15 times of relative fold inductions, respectively.